Irrigation, damming, and streamflow fluctuations of the Yellow River

Zun Yin[1,2], Catherine Ottlé[1], Philippe Ciais[1], Feng Zhou[3], Xuhui Wang[3], Polcher Jan[2], Patrice Dumas[4], Shushi Peng[3], Laurent Li[2], Xudong Zhou[2,5,6], and Shilong Piao[3]

[1]Laboratoire des Sciences du Climat et de l'Environnement, IPSL, CNRS-CEA-UVSQ, Gif-sur-Yvette, France
[2]Laboratoire de Météorologie Dynamique, IPSL UPMC/CNRS, Paris 75005, France
[3]Sino-French Institute for Earth System Science, College of Urban and Environmental Sciences, Peking University, Beijing 100871, China
[4]Centre de Coopération Internationale en Recherche Agronomique pour le Développement, Avenue Agropolis, 34398 Montpellier CEDEX 5, France
[5]Institute of Industrial Science, The University of Tokyo, Tokyo, Japan
[6]State Key Laboratory of Hydrology-Water Resources and Hydraulic Engineering, Center for Global Change and Water Cycle, Hohai University, Nanjing 210098, China

Correspondence: Z. Yin
(zun.yin@foxmail.com)

Abstract. The streamflow of the Yellow River (YR) is strongly affected by human activities like irrigation and dam regulation. Many attribution studies focused on the long-term trend of streamflows, yet the contributions of these anthropogenic factors to streamflow fluctuations have not been well quantified. This study aims to 1) demonstrate whether the global land surface model ORCHIDEE is able to simulate the streamflows of complex rivers with human activities using a generic parameterization, and 2) quantify the respective roles of irrigation and artificial reservoirs in monthly streamflow fluctuations of the YR from 1982 to 2014 by using ORCHIDEE with a newly developed irrigation module, and an offline dam operation model. Validations with observed discharge near the outlet of the YR demonstrated that model performances improved notably with gradually considering irrigation (mean square error [MSE] decreased 56.9%) and dam regulations (MSE decreased 30.5% further). Irrigation was found to substantially reduce the river streamflows by consuming approximately $242.8 \pm 27.8 \times 10^8$ m^3.yr^{-1} in line with the census data ($231.4 \pm 31.6 \times 10^8$ m^3.yr^{-1}). However, it might lead to a slightly increase of the discharge in the summer if irrigation is widely applied throughout a dry preceding spring. Our analysis revealed that the dam regulation, rather than the change of precipitation, was the primary driver altering streamflow seasonality. Inclusion of dam operation dramatically reduced the MSE of simulated discharge by $\geq 48.4\%$ compared to the simulation only considering irrigation, and increased the predictability of water storage changes of the LongYangXia and LiuJiaXia reservoirs (correlation coefficient of ~0.9). This study emphasised the importance of irrigation and damming in understanding the streamflow fluctuations in the YR basin. Moreover, other commonly neglected factors, such as multiple medium reservoirs, large irrigation districts (e.g., the

Hetao Plateau), and special management policies during extreme years, were discovered in our study. Related processes should be integrated in models to better project future water resources under climate change and optimize possible countermeasures for sustainable development.

1 Introduction

More than 60% of rivers all of the world are disturbed by human activities (Grill et al., 2019) contributing to approximately 63% of surface water withdrawal (Hanasaki et al., 2018). River water is used for agriculture, industry, drinking water supply, and electricity generation (Hanasaki et al., 2018; Wada et al., 2014), these usages being influenced by direct anthropogenic drivers and by climate change (Haddeland et al., 2014; Piao et al., 2007, 2010; Yin et al., 2020; Zhou et al., 2020). In order to meet the fast-growing water demand in populated areas and to control floods (Wada et al., 2014), reservoirs have been built up for regulating the temporal distribution of river water (Biemans et al., 2011; Hanasaki et al., 2006) leading to a massive perturbation of the variability of river streamflows. In the mid-northern latitudes regions where a decrease of rainfall is observed historically and projected by climate models (Intergovernmental Panel on Climate Change, 2014), water scarcity will be further exacerbated by the growth of water demand (Hanasaki et al., 2013) and by the occurrence of more frequent extreme droughts (Seneviratne et al., 2014; Sherwood and Fu, 2014; Zscheischler et al., 2018). Thus how to adapt and improve river management under different challenges is a crucial question for sustainable development, which requires comprehensive understanding of the impacts of human activities on river flow dynamics particularly in regions under high water stress (Liu et al., 2017; Wada et al., 2016).

The Yellow River (YR) is the second longest river in China. It flows across arid, semi-arid, and semi-humid regions, and it covers intensive agricultural zones containing about 107 million inhabitants (Piao et al., 2010). With 2.6% of total water resources in China, the Yellow River Basin (YRB) irrigates 9.7% of the croplands of China (http://www.yrcc.gov.cn). More importantly, underground water resources only accounts for 10.3% of total water resources amount in the YRB, outlining the importance of river water for regional water use. A special feature of the YRB is the huge spatio-temporal variation of its water balance. Precipitation concentrates in the flooding season (from July to October) contributing to ~60% of annual discharge, whereas the dry season lasts from March to June accounting for ~10-20%. Numerous artificial reservoirs have been built up to regulate the streamflows intra- and inter-annually in order to control floods and alleviate water scarcity (Liu et al., 2015; Zhuo et al., 2019). The river streamflow is thus highly controlled by human water withdrawals and dam operations, making it difficult to separate the impacts of human and natural factors on the streamflow variability and trends.

Numerous studies assessed the effects of anthropogenic factors on streamflows and water resources in the YRB. By applying a distributed biosphere hydrological model in the YRB, Tang et al. (2008) quantified the contributions of climate change and human activities (irrigation and land cover change) to the annual discharge of the YR at different reaches, and revealed the importance of human activities in influencing the low flow. Following studies confirmed anthropogenic impacts as the dominant factor affecting the trend of the YR discharge through modelling comparison or data analysis (Liu and Du, 2017; Liu et al., 2019; Xi et al., 2018). Moreover, Yuan et al. (2018) investigated human-induced local climate change and demonstrated that its impact on extreme streamflows may be largely underestimated. The YRB is one of the major concerns of many global studies as well. For instance, studies from Haddeland et al. (2014); Hanasaki et al. (2018); Wada et al. (2014, 2016) analyzed potential human and climate impacts on the water resources of the YRB. But at the same time, they pointed out the difficulty in simulating YR streamflow due to large intra- and inter-annual climate variability and complicated human activities.

Although those efforts indeed enhanced our understanding to the interactions among human, water resources, and climate change in the YRB, most of them only focused on the attributions to the long-term trend at annual and decadal scales. How human activities affect intra-annual fluctuations of the streamflows is still not well clarified or quantified, which may mainly affect policies and regional economic activities. Moreover, the impacts of dam operations, as a key factor affecting streamflow seasonality, are not well isolated from other anthropogenic effects in the studies of the YRB. Although there are a set of dam models developed from different perspectives, such as agent-based model River Wave (Humphries et al., 2014) and basin-specific model Colorado River Simulation System (Bureau of Reclamation, 2012), the dam module in many global hydrological studies are based on the work of Hanasaki et al. (2006), which simulates dam operations based on different purposes of reservoirs with adjustment to climate variation. These models are widely applied in global hydrological studies, in which the YRB is one of their major concerns. However, the performances of them in the YRB are always low (Hanasaki et al., 2018; Wada et al., 2014, 2016). Although large uncertainties among model simulations are addressed (Haddeland et al., 2014; Liu et al., 2019), rare studies focus on the YRB to demonstrate where the errors of simulations from due to lack of data. Moreover, the validation periods of many modelling studies started from 1960~1970 to 2000~2010 (Haddeland et al., 2014; Hanasaki et al., 2018; Liu et al., 2019; Tang et al., 2008; Wada et al., 2016) whereas several large reservoirs started regulation much later (e.g., LongYangXia in 1986 and XiaoLangDi in 1999). Such high proportions of observed streamflows rarely affected by reservoirs ($\geq 40\%$) probably cannot guarantee the abilities of models in simulating reservoir operations being correctly evaluated. Thus it is crucial to zoom in the reservoir-dominated period of the YRB to demonstrate the impacts of reservoirs on flow fluctuations under validation by observed dam operations.

Many model studies are able to provide reliable estimation of river discharges but related physical processes are not fully represented. For instance, some model studies require extra observed data as inputs (e.g., leaf area index (LAI), evapotranspiration, etc). Moreover, many biophysical processes (e.g., photosynthesis, LAI dynamics, crop phenology), which tightly couple with evapotranspiration, surface energy balances, and irrigation demands, are rarely considered in Global Hydrological Models (GHM). These missing processes are not important for hydrological studies using historical data and short-term forecast. However, they are probably non-negligible for long-term projections (Duethmann et al., 2020), especially in regions where ecosystems react strongly to climate change through the hydrological cycle (de Boer et al., 2012; Lian et al., 2020; Zhu et al., 2016).

In our previous study, Xi et al. (2018) utilized 0.1° hypo-resolution atmospheric forcing of China (Chen et al., 2011) to drive the land surface model ORCHIDEE (ORganizing Carbon and Hydrology in Dynamic EcosystEms) in aim to attribute the trends of main China's river streamflows to several natural and anthropogenic factors. Due to lack of representation of crop and irrigation processes, simulated results are consistent to the naturalized streamflows of the YR, however much higher than the observations. By developing a new crop-irrigation module in ORCHIDEE (Wang et al., 2016; Wang, 2016; Wu et al., 2016; Yin et al., 2020), we were able to provide precise estimation of crop phenology, yield and irrigation amount at both local and national scales (Wang et al., 2017; Yin et al., 2020). More importantly, ORCHIDEE-estimated irrigation accounts for potential ecological and hydrological impacts (e.g., physiological response of plants to climate change and short term drought episodes on soil hydrology) with respect to other land surface models and global hydrological models. In a study focusing

on China (Yin et al., 2020), ORCHIDEE estimated irrigation withdrawal coincided well with census data (provincial-based spatial correlations are ~0.68), and successfully explained the decline of total water storage in the YRB. Simultaneously, a simple dam operation model was developed to simulate the change of water storages in the main artificial reservoirs. It is based on a targeted operation plan, which relies on the regulation capacity of the reservoir and historical simulated discharge, with flexibility to climate variation. The effects of artificial reservoirs on streamflows could then be studied, and isolated from the effect of climate variability and irrigation trends. Moreover, different from classical approaches separating the YRB into up, middle, and down streams (Tang et al., 2008; Zhuo et al., 2019), we propose to further divide both the up and middle streams into sub-sections based on the locations of five key gauging stations (Fig. 1). This approach splits the regions with/without big reservoirs (or large irrigation areas) in the up and middle streams, which simplifies the assessment of the roles of irrigation and damming on streamflow disturbances of the YR.

Before its integration in ORCHIDEE, the dam model should be validated offline. In this study, both ORCHIDEE and dam model are applied on the YR from 1982 to 2014 in order to: 1) demonstrate whether ORCHIDEE and the dam model, with generic parameterizations, are able to reproduce streamflow fluctuations of the YR with human perturbations; and 2) qualify and quantify the impacts of irrigation and dam regulation on the fluctuations of monthly streamflows. We first introduce the ORCHIDEE model and the simple dam model in Sect. 2.1. Then the algorithm estimating sub-sectional water balances is described in Sect. 2.2, followed by datasets, simulation protocol, and metrics for evaluation in Sect. 2.3-2.5. Results are shown in Sect. 3 and limitations are discussed in Sect. 4.

2 Methodology

2.1 Modelling irrigation and dam regulation

2.1.1 Irrigation in ORCHIDEE

ORCHIDEE is a physical process-based land surface model that integrates hydrological cycle, surface energy balances, carbon cycle, and vegetation dynamics by two main modules. The SECHIBA (surface-vegetation-atmosphere transfer scheme) module simulates the dynamics of water cycle, energy fluxes, and photosynthesis at 0.5 hour time interval, which are used by the STOMATE (Saclay Toulouse Orsay Model for the Analysis of Terrestrial Ecosystems) to estimate vegetation and soil carbon cycle at daily time step. The ORCHIDEE used in this study is a special version with newly developed crop and irrigation module (Wang et al., 2017; Wu et al., 2016; Yin et al., 2020). The novel crop module includes specific parameterizations for three main staple crops: wheat, maize, and rice, which are calibrated over China by observations (Wang, 2016; Wang et al., 2017). It is able to simulate crop carbon allocation, different phenological stages as well as related managements (e.g., planting date, rotation, multi-cropping, irrigation, etc).

Irrigation amount is simulated in the land surface model ORCHIDEE (Wang, 2016; Wang et al., 2017) as the minimum between crop water requirements and water supply. The plant water requirements are defined according to the choice of irrigation techniques, namely minimizing soil moisture stress for flooding, sustaining plant potential evapotranspiration for

dripping, and maintaining the water level above the soil surface during specific months for paddy irrigation. Each crop being grown on a specific soil column (in each model grid-cell) where the water and energy budgets are independently resolved. The water resources in ORCHIDEE account for three water reservoirs: 1) the stream reservoir indicates streamflows; 2) the fast reservoir indicates surface runoff; and 3) the slow reservoir indicates total deep drainage, the order of which indicates the priorities of water reservoirs considered for irrigation. As long-distance water transfer is not taken into account, streams only supply water to the crops growing in the grid-cell they cross, according to the river routing scheme of the ORCHIDEE model (Ngo-Duc et al., 2007). Since reservoirs are not modelled, irrigation may be underestimated where reservoirs regulation stores water in months without irrigation demand to be released it in months with irrigation demand. Transfer from reservoirs, lakes or local ponds to adjacent cells are not considered which should further lead to an underestimation of irrigation demand, dependent on the cell size. Details of the coupled crop-irrigation module of ORCHIDEE are fully described in Yin et al. (2020).

2.1.2 Dam regulation model

To account for the impacts of dam regulation on streamflow (Q) seasonality, we developed a dynamic dam water storage module based on only two simple rules, reducing flood peaks and guaranteeing baseflow. This simple module depends on simulated inflows only and is thus independent from irrigation demands. It has been developed for the main reservoirs of the YRB (e.g., LongYangXia, LiuJiaXia, and XiaoLangDi) to assess the effect of water management rules on streamflows. Different from Biemans et al. (2011); Hanasaki et al. (2006), we primarily consider the ability of reservoirs in regulating river flow seasonality. It means that the targeted baseflow and flood control of our model are not fixed proportions of mean annual discharge, but depends on the regulation capacity of reservoirs ($C_{\max}$). Firstly, similar to Voisin et al. (2013), multi-year averaged monthly discharge (Q_{s}) is calculated based on simulations. To include the potential impacts of climate change on reservoir regulation, here we only consider the latest past 10-year simulations, as:

$$Q_{\mathrm{s},i} = \frac{1}{N} \sum_{j}^{j \in N} Q_i^j. \tag{1}$$

Here $Q_{\mathrm{s},i}$ [$\mathrm{m}^3.\mathrm{s}^{-1}$] is multi-year averaged monthly discharge of month i; j is year index; N is number of year accounted; For a upcoming year j, we only use the historical simulations (maximum latest ten years) to calculate Q_{s}.

Secondly, we evaluate the targeted water storage change ΔW_{t} and monthly discharge Q_{t} considering the regulation capacity of each reservoir. As shown in Fig. S1, one year can be divided into two periods by comparing Q_{s} with $\bar{Q}_{\mathrm{s}}$. The longest continuous months with $Q_{\mathrm{s}} > \bar{Q}_{\mathrm{s}}$ is the recharging season for reservoirs, and the rest is the releasing season. The amount of water stored during the recharging season (blue region in Fig. S1), which is determined by $C_{\max}$, will be used during the

releasing season (red regions in Fig. S1). The ΔW_{t} and Q_{t} can be estimated by:

$$k = \min\left(\frac{C_{\max}}{\alpha \sum_{i \in \text{Recharge}} Q_{\mathrm{s},i}}, k_{\max}\right), \tag{2}$$

$$\Delta W_{\mathrm{t},i} = k\alpha\left(Q_{\mathrm{s},i} - \bar{Q}_{\mathrm{s}}\right) + \bar{Q}_{\mathrm{s}}, \tag{3}$$

$$Q_{\mathrm{t},i} = Q_{\mathrm{s},i} - \Delta W_{\mathrm{t},i}/\alpha. \tag{4}$$

Here k [-], varying between 0 and $k_{\max}$ (=0.7), indicates the ability of reservoir in disturbing streamflow seasonality. It is a ratio of the maximum regulation capacity of the reservoir $C_{\max}$ [10^8 m^3] over the discharge amount throughout the recharging season. α (0.0263) converts monthly discharge to water volume. Assuming that the water storage of the reservoir reaches $C_{\max}$ at the end of the recharging season, we can calculate targeted water storage W_{t} by using ΔW_{t}.

Finally, the variation of the actual water storage of the reservoir ΔW is a decision regarding actual monthly discharge, current water storage, Q_{t}, ΔW_{t}, and W_{t}. During the releasing season, ΔW is calculated as:

$$\Delta W_i = \begin{cases} -W_i \dfrac{(-\Delta W_{\mathrm{t},i})}{W_{\mathrm{t},i}} & \text{if } W_i \le W_{\mathrm{t},i}; \quad (5a) \\ \Delta\tilde{W}_i - \left[\left(W_i + \Delta\tilde{W}_i\right) - \left(W_{\mathrm{t},i} + \Delta W_{\mathrm{t},i}\right)\right] & \text{if } W_i > W_{\mathrm{t},i} \text{ and } \Delta\tilde{W}_i > \Delta W_{\mathrm{t},i}; \quad (5b) \\ \Delta W_{\mathrm{t},i} - \left(W_i - W_{\mathrm{t},i}\right) & \text{if } W_i > W_{\mathrm{t},i} \text{ and } \Delta\tilde{W}_i \le \Delta W_{\mathrm{t},i}. \quad (5c) \end{cases}$$

Here $\Delta\tilde{W}_i = \alpha Q_i - (\alpha Q_{\mathrm{t},i} - \Delta W_{\mathrm{t},i})$. It is the expected release amount to make river discharge equal to the targeted discharge after reservoir regulation. If current water storage is less than the targeted value (the case of Eq. 5a), the ΔW_i is calculated by the W_i with a proportion of $\Delta W_{\mathrm{t},i}$ over $W_{\mathrm{t},i}$. If the current storage is more than the targeted value (the cases of Eq. 5b and 5c), the reservoir can release more water based on a balance between the targeted water storage change $\Delta W_{\mathrm{t},i}$ and the targeted water storage at the next time step $W_{\mathrm{t},i}$ (represented by $\Delta\tilde{W}_i$). Note that all water storage change variables are negative throughout the releasing season.

During the recharging season, we can calculate the ΔW_i as:

$$\Delta W_i = \begin{cases} \max\left(\min\left(W_{\mathrm{t},i} + \Delta W_{\mathrm{t},i} - W_i, \alpha Q_i\right), 0\right) & \text{if } W_i > W_{\mathrm{t},i}; \quad (6a) \\ \min\left(\Delta W_{\mathrm{t},i} + \left(W_{\mathrm{t},i} - W_i\right), \alpha Q_i\right) & \text{if } W_i \le W_{\mathrm{t},i}. \quad (6b) \end{cases}$$

If current water storage is larger than the targeted value (Eq. 6a), we will try to recharge a volume of water to make $W_{i+1} = W_{\mathrm{t},i+1}$. If current water storage is less than the targeted value (Eq. 6b), we decide to recharge additional water volume besides the $\Delta W_{\mathrm{t},i}$.

ΔW is then applied as a correction of simulated discharge to generate actual monthly discharge using the following equation:

$$\hat{Q}_{\mathrm{sim},i} = Q_{\mathrm{sim},i} - \frac{1}{\alpha}\Delta W_i. \tag{7}$$

Here $\hat{Q}_{\text{sim}}$ [$\text{m}^3.\text{s}^{-1}$] is the simulated regulated discharge; Q_{sim} [$\text{m}^3.\text{s}^{-1}$] is the simulated monthly discharge. Note that this model is a simplified representation of dam management, because it ignores the direct coupling between water demand and irrigation water supply from the cascade of upstream reservoirs. This approach implies that, with a regulated flow, demands will be able to be satisfied and floods to be avoided without being more explicit. A complete coupling of demand, flood, and reservoir management is difficult to implement in the land surface model in absence of data about the purpose and management strategy of each dam, given different possibly conflicting demand of water for industry and drinking versus cropland irrigation.

Before performing the simulation, we estimate the maximum regulation capacity of each study reservoir in each river sections shown in Fig. 1. Table 1 lists collected information of the main reservoirs on the YR. Only large reservoirs like LongYangXia (LYX), LiuJiaXia (LJX), and XiaoLangDi (XLD) are considered in our model because of their huge C_{max}.

2.2 Sub-section diagnosis

Figure 1 shows the YRB and main gauging stations used in this study. To effectively use Q_{obs} for investigating impacts of irrigation and dam regulations on the streamflows of different river sections, we divided the YRB into five sub-sections (R_i, $i \in [1, 5]$, Fig. 1) with an outlet at each gauging station. Thus we can evaluate the water balance in R_i by:

$$\frac{\Delta \text{TWS}_i}{\Delta t} = P_i - \text{ET}_i + \frac{Q_{\text{in},i} - Q_{\text{out},i}}{A_i}. \tag{8}$$

Where Δt is time interval; ΔTWS_i [mm] is change of total water storage in specific R_i; P_i [$\text{mm}.\Delta t^{-1}$] is precipitation in R_i; ET_i [$\text{mm}.\Delta t^{-1}$] is evapotranspiration in R_i; A_i [m^2] is area of R_i. $Q_{\text{in},i}$ and $Q_{\text{out},i}$ [$\text{m}^3.\Delta t^{-1}$] are inflow and outflow respectively. In addition, $q_i = Q_{\text{out},i} - Q_{\text{in},i}$ indicates the contribution of R_i to the river discharge, that is the sub-section discharge. This term can be negative if local water supply (e.g., precipitation and groundwater) cannot meet water demand. A conceptual figure of the water balance of a sub-section is shown at the top left of Fig. 1.

2.3 Datasets

Observed monthly discharge (Q_{obs}) from the gauging stations shown in Fig. 1 are used to evaluate the simulations. Several precipitation (P) and evapotranspiration (ET) datasets were selected to evaluate simulated water budgets in each sub-section. The 0.5° 3-hourly precipitation data from GSWP3 (Global Soil Wetness Project Phase 3) is based on GPCC v6 (Global Precipitation Climatology Centre (Becker et al., 2013)) after bias correction with observations. The MSWEP (Multi-Source Weighted-Ensemble Precipitation) is a 0.25° 3-hourly P product integrating numerous in-situ measurements, satellite observations, and meteorological reanalysis (Beck et al., 2017). Three ET datasets are chosen for their potential ability to capture the effect of irrigation disturbance on ET (Yin et al., 2020) (noted as ET_{obs}). GLEAM v3.2a (Global Land Evaporation Amsterdam Model, (Martens et al., 2017)) provides 0.25° daily ET estimations based on a two-soil layer model in which the top soil moisture is constrained by the ESA CCI (European Space Agency Climate Change Initiative) Soil Moisture observations. The FLUXCOM model (Jung et al., 2009) upscales ET data from a global network of eddy covariance towers measurements into a global 0.5° monthly ET product. Since these towers do not cover irrigated systems, ET from irrigation simulated by the LPJml (Lund-Postam-Jena managed Land) is added to ET from non-irrigated systems. The PKU ET product estimates 0.5°

monthly ET by water balances at basin scale integrating FLUXNET observations to diagnose sub-basin patterns by a Multiple Tree Ensemble approach (Zeng et al., 2014).

2.4 Simulation protocol

The 0.5° half-hourly GSWP3 atmospheric forcing (Kim, 2017) was used to drive ORCHIDEE simulations. Yin et al. (2018) used four atmospheric forcings to drive ORCHIDEE to simulate soil moisture dynamics over China. And the GSWP3-driven simulation provided the best performances based on validations by in-situ measurements and satellite observations. A 0.5° map with 15 different Plant Functional Types (PFTs) containing crop sowing area information for the three PFTs corresponding to the modeled crop (wheat, maize, and rice) is used, based on 1:1 million vegetation map and provincial scale census data of China. Crop planting dates for wheat, maize, and rice are derived from spatial interpolation of phenological observations from Chinese Meteorological Administration (Wang et al., 2017). Soil texture map is from Zobler (1986). Two simulation experiments were performed to assess the impacts of irrigation on river streamflows: 1) NI: no irrigation; 2) IR: irrigated by available water resources. In IR, only surface irrigation is considered in this study (irrigated water is applied on the cropland surface without interception by canopies), which only works during the crop growth period. The soil water stress, a function of profiles of soil moisture and crop root density (up to 2 m depth, (Yin et al., 2020)), is checked every half an hour. When it is less than a target threshold (=1), irrigation will be triggered with amount equal to the deficit of saturated and current soil moisture. To precisely estimate irrigation water consumption (direct water loss from the surface water pool excluding return flow), the deep drainage of the three crop soil columns is turned off in the IR simulation. Simulations start from a 20-year spin-up in 1982 to initialize the thermal and hydrological variables. Then simulations were performed from 1982 to 2014 over the YRB.

The dam operation simulation starts from 1982 with simulated Q from the IR simulation (Q_{IR}) as input. The initial values of W were set to half of the corresponding C_{max}. Considering potential joint regulation of reservoirs, we firstly estimate the total ΔW of all considered reservoirs by using Q_{IR} at HuaYuanKou (outlet of R_4, Fig. 1). Then we estimate the ΔW of LYX and LJX reservoir by using Q_{IR} at LanZhou. The difference between these two ΔW is assumed as the ΔW of XLD reservoir. Simulated ΔW is used to estimate regulated monthly discharge ($\hat{Q}_{\text{IR}}$) as Eq. 7 without time lag (Fig. S2). As huge irrigation water withdrawal occurs in R_3 and R_5 (YRCC, 1998–2014), slightly water recharge of reservoir up reaches may result in negative $\hat{Q}_{\text{IR}}$ at TouDaoGuai and LiJin. To avoid this numerical circumstances due to offline run of the dam model, we corrected all negative $\hat{Q}_{\text{IR}}$ to zero by assuming that the streamflows cannot further drop when all stream water are consumed upstream. The impact of this corrections will be taken into account at other gauging stations downstream.

2.5 Evaluation metrics

Three metrics are used to evaluate the performances of simulated monthly Q. The mean-square error (MSE) evaluates the magnitude of errors between simulation and observations. It can be decomposed into three components (Kobayashi and Salam, 2000):

$$\text{MSE} = \frac{1}{n}\sum_{i=1}^{n}(S_i - O_i)^2 = \text{SB} + \text{SDSD} + \text{LCS}. \tag{9}$$

Where S_i and O_i are simulated and observed values, respectively; n is the number of samples. SB (squared bias) is the bias between simulated and observed values. In this study, SB represents the difference between simulated and observed multi-year mean annual Q. SDSD (the squared difference between standard deviation) relates to the mismatch of variation amplitudes between simulated and measured values. It can reflect whether our simulation can capture the seasonality of Q_{obs}. LCS (the lack of correlation weighted by the standard deviation) indicates the mismatch of fluctuation patterns between simulated and observed values, which is equivalent to inter-annual variation of Q in this study. The formulas of these three components and detailed explanation can be found in Kobayashi and Salam (2000).

The index of agreement ($d \in [0,1]$) is defined as the ratio of MSE and potential error. It is calculated as:

$$d = 1 - \frac{\sum_{i=1}^{n} (O_i - S_i)^2}{\sum_{i=1}^{n} \left(|S_i - \bar{O}| + |O_i - \bar{O}|\right)^2}. \tag{10}$$

$d = 1$ indicates perfect fit, while $d = 0$ denotes poor agreement.

The modified Kling-Gupta Efficiency (mKGE $\in (-\infty, 1]$) is defined as the Euclidean distance of three independent criteria: correlation coefficient r, bias ratio β, and variability ratio γ (Gupta et al., 2009; Kling et al., 2012). It is an improved indicator from the Nash-Sutcliffe Efficiency avoiding heterogeneous sensitivities to peak and low flows, which is crucial for this study that is not only interested in simulating peak flows but also concentrates on base flows regulated by dams for human usage. mKGE is calculated as,

$$\text{mKGE} = 1 - \sqrt{(1-r)^2 + (1-\beta)^2 + (1-\gamma)^2}, \tag{11}$$

$$\beta = \frac{\mu_S}{\mu_O}; \gamma = \frac{\text{CV}_S}{\text{CV}_O}, \tag{12}$$

where r is the correlation coefficient between observed and simulated discharges; μ [$\text{m}^3.\text{s}^{-1}$] and CV [-] are the mean and the coefficient of variation of Q, respectively. These indicators are used for three comparisons: 1) Q_{NI} and Q_{obs}; 2) Q_{IR} and Q_{obs}; 3) $\hat{Q}_{\text{IR}}$ and Q_{obs}.

3 Results

3.1 Hydrological cycles at sub-sectional scale

Figure 2 displays water balances and trends in R_i based on simulated results and observations. P_{GSWP3}, which is consistent with P_{MSWEP}, decreases from 543.6 mm.yr^{-1} (R_1) to 254.2 mm.yr^{-1} (R_3), and then rises until 652.1 mm.yr^{-1} (R_5). The magnitudes of simulated ET (both ET_{NI} and ET_{IR}) have no significant differences with ET_{obs} aggregated over sub-sections R_1 to R_5. Grid cell-based validation shows high agreements between simulated and observed ET across all sub-sections (the lowest mean of correlation coefficients is 0.79 and the highest mean of relative RMSE is 4.9%, Table S1). Except for R_1 where cropland is rare, ET_{IR} accounts for more than 80% of P_{GSWP3} in the YRB with a maximum value of 96.5% in R_3. The difference between ET_{IR}

and ET_{NI} is due to the account of irrigation, which accounts for 9.1% and 8.2% of ET_{NI} in R_3 and R_5 respectively as caused by the large irrigation demand. The impact of irrigation can be detected from sub-sectional discharges ($q_i = (Q_{out,i} - Q_{in,i})/A_i$) as well. For instance, both q_{obs} and q_{IR} are negative in R_3 and R_5, suggesting that local surface water resources cannot meet water usage and upstream discharge is used for irrigation. As irrigation water transfers between grid cells are not represented in our simulations, the non-availability of water locally results in an underestimation of the irrigation amounts explaining why $q_{IR} > q_{obs}$ in R_3 to R_5.

The trends of P and ET are positive but not significant in most R_i during the period 1982–2014 (bottom panel of Fig. 2). However, significant trends can be found in both simulated and observed q in some R_i. The decrease of q_{obs} in R_1 is not captured by the model, neither in q_{NI} nor q_{IR}. This underestimated decrease of river discharge might be linked to decreased glacier melt or increased non-irrigation human water withdrawals, which are ignored in our simulations. In R_2 and R_3, the q_{obs} trends are determined by the joint effects of climate change (e.g., P increase) and human water withdrawals. The trends of q_{IR} show the same direction as that of q_{obs}. In R_5 however q_{obs} increased by 1.67 mm.yr^{-1}, which was not captured by the simulation for q_{IR}. Besides P increase shown here, another possible driver of increasing q_{obs} in R_5 is a decrease of water withdrawal due to the improvement of irrigation efficiency (Yin et al., 2020). Moreover, the water use management may play an important role in the observed positive trends of q_{obs} as well, with the aim to increase the streamflows at the downstream of the YR to avoid discharge cutoff ($Q_{obs} < 1$ m^3.s^{-1}) that occurred in 1990's (Wang et al., 2006).

Irrigation not only influences annual discharge in the YR, but also affects its intra-annual variation. In general, the discharge yield, (Y_Q, defined by the sum of surface runoff and drainage) of all grid cells in NI should be higher than that in IR because our irrigation model harvests the stream water reservoirs which is a fraction of drainage and runoff. However, our simulations show that $Y_{Q,NI}$ can be less than $Y_{Q,IR}$ (Fig. S3) at the beginning of monsoon season. This is because irrigation keeps soil moisture (SM) higher than SM without irrigation in July in R_4 and R_5 (Fig. S3d and S3e), which in turn promotes Y_Q because the soil water capacity is lower and a larger fraction of P goes to runoff. This mechanism highlighted that irrigation could enhance the heterogeneity of water temporal distribution and may reinforce upcoming floods after a dry season.

3.2 Comparison between observed and simulated Q

Figure 3 illustrates time series of annual discharge and of the seasonality of monthly discharge. Our simulations underestimate Q_{obs} at TangNaiHai in R_1 because we miss glacier melt. After LanZhou, the magnitudes of Q_{IR} coincide very well with that of Q_{obs}, indicating that irrigation strongly reduces the annual discharge of YR by as much as 64% until R_5. However, the seasonality of monthly Q_{IR} is quite different from that of Q_{obs} (Fig. 3f-3j). Despite a good match between annual Q_{IR} and Q_{obs} our model without dams produces an underestimation of Q in dry season and an overestimation of Q in flood season. Such a mismatch of Q seasonality is likely caused primarily by dam regulation ignored in the model. The locations of several big reservoirs are shown in the bottom panel of Fig. 1 and related information are listed in Table 1. Before the operation of the LongYangXia dam which has a regulation capacity of 193.5×10^8 m^3 (green bar in Fig. 4b), the peaks of monthly Q_{NI} at LanZhou were slightly lower than the peaks of Q_{obs} in R_2 (Fig. 4b), as well as the case at TangNaiHai (Fig. 4a), possibly due to lack of glacier melt in the model for this upper sub-section of the YRB in our simulation. But after the construction

of the LongYangXia reservoir in 1986, modeled peak Q_{NI} became systematically higher than the peak of Q_{obs} each year, suggesting that the construction of this dam caused the observed peak reduction (Fig. 4b). Moreover, the seasonality of Q_{obs} changed dramatically in period of 1982-2014, but no similar trend was found in monthly P (Fig. S4), suggesting that reservoir regulation is the primary driver of the observed shift in seasonal streamflow variations of the YRB from 1982 to 2014.

Reservoirs can also affect inter-annual variations of Q as well, although less than the seasonal variation. For instance, TongGuan and XiaoLangDi are two consecutive gauging stations upstream and downstream the reservoir of XiaoLangDi in R_4 (Fig. 1). The annual Q_{obs} at the two stations shows different features after the construction of the XiaoLangDi reservoir in 1999.

Figure 5 shows monthly time series of Q_{obs}, Q_{IR}, and $\hat{Q}_{\mathrm{IR}}$ (see Sect. 2.1.2) at each gauging station. Discharge fluctuations are successfully improved in $\hat{Q}_{\mathrm{IR}}$. Especially the baseflow of $\hat{Q}_{\mathrm{IR}}$ coincides well with that of Q_{obs} during winter and spring. The only exception occurs at LiJin, where $\hat{Q}_{\mathrm{IR}}$ overestimates the discharge from January to May. In fact, the water release from XLD during this period would be withdrawn for irrigation and industry in R_5. However, our offline dam model is not able to simulate the interactions, leading to the overestimation.

The dam model is successful in flood control as well. At LanZhou, although $\hat{Q}_{\mathrm{IR}}$ underestimates the peak flows due to the bias of the simulated mean annual discharge (Fig. 3b), its seasonality is much smoother than that of Q_{IR}. Indeed, such underestimation is also affected by special water management during extreme years. From 2000 to 2002, the YRB experienced severe droughts with 10~15$\%$ precipitation less than usual, leading to a decrease of surface water resource as much as 45$\%$ (Water Resources Bulletin of China, http://www.mwr.gov.cn/sj/tjgb/szygb/). To guarantee base flow, a set of temporal policies were applied (e.g., reducing water withdrawn, increasing water price, releasing more water from reservoirs, etc). However, those measures are not accounted in the model. Thus higher irrigation demand during dry years promotes the underestimation of the river discharge. From TouDaoGuai to LiJin, the floods from August to October are dramatically reduced by the dam model. Nevertheless, the peaks are still overestimated in $\hat{Q}_{\mathrm{IR}}$. It might be due to numerous medium reservoirs ignored by our model (203 medium reservoirs until the end of 2014 (YRCC, 1998–2014)). In our simulation, 326.5×10^8 m^3 regulation capacity is considered, which only accounts for 45$\%$ of total storage capacity (720×10^8 m^3 (Ran and Lu, 2012)). Moreover, the five irrigation districts (http://www.yrcc.gov.cn/hhyl/yhgq/, (Tang et al., 2008)), a special irrigation system in the YRB, could contribute to flood reduction. For instance, the Hetao Plateau is the traditional irrigation district. Its hydraulic system can divert river water into its complicated irrigation network ([106.5–109°E]×[40.5–41.5°N] in Fig. 1) by water level difference during the flood season. This no-dam diversion system at the Hetao Plateau can take 50×10^8 m^3 from the YR per year, accounting for 14$\%$ annual discharge in R_3.

Simulated ΔW in R_2 is verified by comparing to observations (Jin et al., 2017) (left panel of Fig. 6) suggesting that our dam model is able to capture the seasonal variation of ΔW ($r = 0.9$, $p < 0.001$). In the case of XiaoLangDi where the correlation is smaller ($r = 0.34$, $p = 0.28$; right panel of Fig. 6), the mismatch could be explained by sediment regulation procedures, given that this reservoir releases a huge amount of water in June for reservoir cleaning and sediment flushing downstream (Baoligao et al., 2016; Kong et al., 2017; Zhuo et al., 2019), a process not taken into account in our simple dam model. Moreover, because we ignored numerous medium reservoirs, the simulated water recharge during the flood season could be overestimated.

Figure 7 illustrates the model performances with different metrics in different R_i. The results show that MSE increases considerably from R_1 to R_5, implying accumulated impacts of ignored error sources in increasing the error of modeled Q when going downstream in the entire catchment. Most likely those error sources are omission errors of anthropogenic factors such as drinking and industrial water removals, but also of natural origin such as the role of riparian wetlands and floodplains (e.g., the SanShengGong water conservancy hub), and the non-represented small streams in the routing of ORCHIDEE (e.g., the irrigation system at the Hetao Plateau). From the decomposition of MSE, we found that adding irrigation in the model removes most of the bias in the average magnitude Q by reducing the SB error term of MSE. The only exception occurs at LanZhou, where SB increases in IR consequently leading to higher MSE. It is due to the underestimation of Q upstream (Fig. 3a). Thus the Q_{IR} is lower at LanZhou and enlarges the SB. On the other hand, adding the reservoir regulations contribute to improve the phase variations of Q which are dominated by the phase of the seasonal cycle, by reducing the SDSD error term. Nevertheless, the LCS error term indicating the magnitude of the variability, mainly at inter-annual time scales, has no significant improvement with the representation of irrigation and dam regulations. It is because some of reservoirs are able to regulate Q inter-annually (Table 1), which can be observed from Fig. 4c. However, related operation rules are unclear and are not implemented in our dam model. Improvements were found in d as well, which demonstrates that the way human effects on Q of the YR were modeled brings more realistic results, despite ignoring the direct effect of irrigation demand on reservoir release, and ignored industrial and domestic water demands. The mKGE reveals significant increase after considering dam operations (Fig. 7d). Particularly at LanZhou and HuaYuanKou, the mKGE of $\hat{Q}_{\mathrm{IR}} \sim Q_{\mathrm{obs}}$ increases 0.86 and 1.11 than that of $Q_{\mathrm{IR}} \sim Q_{\mathrm{obs}}$, respectively. Note that the mKGEs of $Q_{\mathrm{IR}} \sim Q_{\mathrm{obs}}$ are smaller than that of $Q_{\mathrm{NI}} \sim Q_{\mathrm{obs}}$ from R_2 to R_4, because irrigation decreases the mean annual discharge of Q_{IR}, which further increases the CV_S leading to worse γ in mKGE (Eq. 11).

4 Discussion

This study validated the performances of the ORCHIDEE land surface model and a dam operation model in simulating hydrological processes in the YRB, and quantified the impacts of irrigation and dam operation on the fluctuations of the YR streamflow. Simulated hydrological components were compared to observations in different sub-sections with fair agreement (e.g., $4.5 \pm 6.9\%$ for ET). Irrigation mainly affects the magnitude of annual discharge by consuming $242.8 \pm 27.8 \times 10^8$ m^3.yr^{-1} consistent to census data with $231.4 \pm 31.6 \times 10^8$ m^3.yr^{-1} (YRCC, 1998–2014). As the water of YR is reaching the limit of usage (Feng et al., 2016), we did not find any significant effect of irrigation on streamflow trends. Instead of increasing river water withdrawals, the growing water demand appeared to have been balanced by improving water use efficiency during the study period (Yin et al., 2020; Zhou et al., 2020). Our simulation reveals that the impact of irrigation on streamflow may be positive under special situations, which was also shown in one previous study (Kustu et al., 2011). However, different from the irrigation-ET-precipitation atmospheric feedback mechanisms found by Kustu et al. (2011), we demonstrated that irrigation may significantly increase soil moisture and promote runoff yield during the following wet season. It implies that irrigation in such landscapes may reinforce the magnitude of floods during the rainy season by a higher legacy soil moisture.

Dams strongly regulate the temporal variation of streamflows (Chen et al., 2016; Li et al., 2016; Yaghmaei et al., 2018). By including simple regulation rules depending on inflows, our dam model explained about 48–77% of the simulation error (MSE in Fig. 7), especially for SDSD which is dominated by seasonal modulation from dams on the river discharge. Moreover, we confirmed that the change of Q_{obs} seasonality during the study period is not due to climate change (Fig. S4), but is determined by dam operations (Wang et al., 2006). Big dams, like the LongYangXia, LiuJiaXia, and XiaoLangDi, are able to regulate streamflows inter-annually (Wang et al., 2018) in order to smooth the inter-annual distribution of water resources in YRB (Piao et al., 2010; Wang et al., 2006; YRCC, 1998–2014). However, corresponding operation rules are unclear and were not implemented explicitly in the simple dam model. The error corresponding to inter-annual variation (LCS in MSE in Fig. 7) was not reduced by including our simulation of dams. In the dam model, some functions of reservoirs, such as providing irrigation supply, industrial and domestic water, electricity generation, and flood control (Basheer and Elagib, 2018) are not explicitly represented. Particularly the XiaoLangDi dam carries a distinctive water-sediment mission, which scours sediments at downstream of the YR by creating artificial floods in June (Kong et al., 2017; Zhuo et al., 2019). These functions are associated with many socioeconomic factors and drivers leading to competing demands for water (e.g., policies, electricity price, water price, land use change, irrigation techniques, water management techniques, and dams inter-connection), which could be better understood and implemented into integrated hydrological models to project future water resources dynamics for sustainable development.

Our simulations ignored potential impacts of dams and reservoirs on local climate (Degu et al., 2011). The sum of water area of several artificial reservoirs (LongYangXia, LiuJiaXia, BoHaiWan, SanShengGong, and XiaoLangDi) is approximately $1056\,\text{km}^2$, which is larger than the 10th largest natural lake in China (Lake Zhari Namco with $996.9\,\text{km}^2$ surface area). These water bodies can also significant influence local energy budgets. And related water loss from reservoir evaporation may be considerable especially in arid and semi-arid area (Friedrich et al., 2018; Shiklomanov, 1999), which should be taken into account in future studies. Besides, the five large irrigation districts (http://www.yrcc.gov.cn/hhyl/yhgq/) could dramatically alter the local climate as well. For instance, the Hetao Plateau takes about $50\times10^8\,\text{m}^3$ from the YR every year during the flood season. Its irrigation area is $5740\,\text{km}^2$ with an evapotranspiration rate ranging between 1200~1600 mm.yr^{-1}. However, as these irrigation districts divert river water without dams or with multiple medium dams, they are not taken into account in most YR studies. Another non-negligible factor in the case of YR is sedimentation, which reduces the regulation capacities of reservoirs and weakens streamflow regulation by human. For instance, the total capacity of QingTongXia declined from 6.06 to $0.4\times10^8\,\text{m}^3$ since 1978 due to sedimentation. Therefore, how land use change and evolution of natural ecosystems affect sediment load and deposition is another key factor to project dams disturbances on streamflows in the YRB.

Simulating anthropogenic disturbances to river streamflows is challenging. In the case of the YR, well calibrated models can provide accurate naturalized discharge simulations for short-term prediction with Nash-Sutcliffe Efficiency (NSE) as high as 0.9 (Yuan et al., 2016). However, when considering the impacts of irrigation and dams, the NSE values of simulations are much worse. For instance, the simulation considering anthropogenic effects from Hanasaki et al. (2018) had lower NSE than the simulation with only natural processes. Similarly, Wada et al. (2014) showed NSE decrease after considering anthropogenic factors in the YRB. These NSE decreases were interpreted due to the complexity of the YRB under the impacts of human ac-

tivities and climate variation. However, the NSE of naturalized discharges is incomparable to the NSE of regulated discharges. Even if the model can perfectly simulate the reservoir operations, the NSE of naturalized discharges is certainly larger than that of regulated discharges from the same model, if you accept the assumption that reservoir operations reduce the variation of river streamflows (a simple proof is available in Sect. A in the online supplement). In fact, our simulated patterns are very similar with a set of simulations by GHMs (Fig. S2 from Liu et al. (2019)). By gradually considering anthropogenic factors (irrigation and dam operations), the performances of our simulations increase dramatically according to all the three metrics.

Intensive calibrations or using a suite of observed inputs can allow catchment-scale studies to provide high-accurate simulated discharges for short-term flood forecast. However, the parameterizations are not generic for broad application in other catchments that lack information in particular (Nash and Sutcliffe, 1970). Moreover, insensitive calibrations are not helpful to reveal important mechanisms missed in the model. Without these crucial mechanisms, models hardly to extrapolate their knowledge to predict extreme events and future flood characters under climate change (Duethmann et al., 2020). Unlike them, one aim of our modelling study is to demonstrate interactive mechanisms in a physical-based land surface model. Although mismatches exist in the simulated discharges, they are unlikely caused by the false representations of physical laws or unsuitable parameterization in our model, because other simulated hydrological variables coincide well with observations in the YRB (e.g., soil moisture dynamics (Yin et al., 2018), naturalized river streamflows (Table S1 in Xi et al. (2018)), leaf area index (Section S2 in Xi et al. (2018)), amount and trend of irrigation withdrawals (Yin et al., 2020), trends of total water storage (Section 3.4 in Yin et al. (2020)), and ET (Table S1)). On the contrary, these mismatches draw our attention to some key mechanisms overlooked in most models. For instance, our model underestimates the annual discharge at LanZhou in the period 2000–2002 (Fig. 3b), during which $\hat{Q}_{\mathrm{IR}}$ was almost negatively correlated to the Q_{obs} (Fig. 5a). From China Water Resources Bulletin (2000–2002, http://www.mwr.gov.cn/sj/tjgb/szygb/), we find that to avoid discharge cutoff ($Q < 1\,\mathrm{m}^3.\mathrm{s}^{-1}$) irrigation and hydropower are strictly restricted throughout the droughts. It suggests that integrated catchment management plays an important role in river flow variation, especially for extreme years. Obviously, models are not able to reproduce this special reaction by over calibration, if the related mechanisms are missing. All in all, mismatches may be useful if they can help us to discover important mechanisms missed before (Duethmann et al., 2020; Scanlon et al., 2018), which is crucial to improve the robustness of a model for future projection.

5 Conclusions

A land surface model ORCHIDEE and a newly developed dam model are utilized to simulate the streamflow fluctuations and dam operations in the Yellow River Basin. The impacts of irrigation and dam regulation on streamflow fluctuation of the Yellow River were qualified and quantified in this study by using a process-based land surface model and a dam operation model. Irrigation mainly contributes to the reduction of annual discharge by as much as $242.8 \pm 27.8^{8}\ \mathrm{m}^3.\mathrm{yr}^{-1}$. The shifts of intra-annual variation of the Yellow River streamflows appear not to be caused by climate change, at least not by significant changes of precipitation patterns and land use during the study period, but by the construction of dams and their operation. After considering the impacts of dams, we found that dam regulation can explain about 48–77% of the fluctuations of streamflows.

The effect of dams may be still underestimated because we only considered simple regulation rules based on inflows, but ignored its interactions with irrigation demand downstream. Moreover, our analysis showed that several reservoirs on the Yellow River are able to influence streamflows inter-annually. However, such effects are not quantified due to lack of knowledge of the regulation rules across our study period.

Code and data availability. The code of ORCHIDEE can be assessed via https://forge.ipsl.jussieu.fr/orchidee/wiki. The data used in this study, and the code of the dam operation model, analysis, and plotting can be accessed via https://doi.org/10.5281/zenodo.3979053 (Yin, 2020). The GLEAM ET data can be downloaded from http://gleam.eu (Martens et al., 2017). The MSWEP precipitation data and the PKU ET are available from http://gloh2o.org (Beck et al., 2017) and Zhenzhong Zeng (Zeng et al., 2014), respectively, which can be obtained upon reasonable requests.

Author contributions. ZY, CO, and PC designed this study; ZY and XW contributed to the model developments; ZY, FZ, XW, and XZ prepared observed datasets; ZY performed model simulations and primary analysis, and drafted the manuscript; all authors contributed to results interpretation, additional analysis, and manuscript revisions.

Competing interests. The authors declare that they have no conflict of interest.

Acknowledgements. We would like to thank the editor and the two anonymous referees for their insightful comments and efforts. We are gratefully acknowledge the GLEAM team, the FLUXCOM team, Hyungjun Kim, Hylke Beck, and Zenzhong Zeng for their selfless sharing of their datasets.

Financial support. This study was supported by the National Natural Science Foundation of China (grant number 41561134016), the CHINA-TREND-STREAM French national project (ANR Grant No. ANR-15-CE01-00L1-0L), and the National Key Research and Development Program of China (2016YFD0800501).

References

Baoligao, B. Y., Xu, F. R., Chen, X. R., Wang, X. Y., and Chen, W. X.: Acute impacts of reservoir sediment flushing on fishes in the Yellow River, Journal of Hydro-Environment Research, 13, 26–35, https://doi.org/10.1016/j.jher.2015.11.003, https://linkinghub.elsevier.com/retrieve/pii/S1570644316000022, 2016.

Basheer, M. and Elagib, N. A.: Sensitivity of Water-Energy Nexus to dam operation: A Water-Energy Productivity concept, Science of the Total Environment, 616-617, 918–926, https://doi.org/10.1016/j.scitotenv.2017.10.228, http://linkinghub.elsevier.com/retrieve/pii/S0048969717329467, 2018.

Beck, H. E., van Dijk, A. I. J. M., Levizzani, V., Schellekens, J., Miralles, D. G., Martens, B., and de Roo, A.: MSWEP: 3-hourly 0.25° global gridded precipitation (1979–2015) by merging gauge, satellite, and reanalysis data, Hydrology and Earth System Sciences, 21, 589–615, https://doi.org/10.5194/hess-21-589-2017, https://www.hydrol-earth-syst-sci.net/21/589/2017/, 2017.

Becker, A., Finger, P., Meyer-Christoffer, A., Rudolf, B., Schamm, K., Schneider, U., and Ziese, M.: A description of the global land-surface precipitation data products of the Global Precipitation Climatology Centre with sample applications including centennial (trend) analysis from 1901–present, Earth System Science Data, 5, 71–99, https://doi.org/10.5194/essd-5-71-2013, http://www.earth-syst-sci-data.net/5/71/2013/, 2013.

Biemans, H., Haddeland, I., Kabat, P., Ludwig, F., Hutjes, R. W. A., Heinke, J., Von Bloh, W., and Gerten, D.: Impact of reservoirs on river discharge and irrigation water supply during the 20th century, Water Resources Research, 47, https://doi.org/10.1029/2009WR008929, http://doi.wiley.com/10.1029/2009WR008929, 2011.

Bureau of Reclamation: Colorado River Basin Water Supply and Demand Study, Tech. Rep. December, Department of the Interior Bureau of Reclamation, Phoenix, 2012.

Chen, J., Finlayson, B. L., Wei, T. Y., Sun, Q. L., Webber, M., Li, M. T., and Chen, Z. Y.: Changes in monthly flows in the Yangtze River, China – With special reference to the Three Gorges Dam, Journal of Hydrology, 536, 293–301, https://doi.org/10.1016/j.jhydrol.2016.03.008, http://dx.doi.org/10.1016/j.jhydrol.2016.03.008https://linkinghub.elsevier.com/retrieve/pii/S0022169416301135, 2016.

Chen, Y. Y., Yang, K., He, J., Qin, J., Shi, J. C., Du, J. Y., and He, Q.: Improving land surface temperature modeling for dry land of China, Journal of Geophysical Research, 116, D20 104, https://doi.org/10.1029/2011JD015921, http://www.tandfonline.com/doi/abs/10.1080/10643380902800034http://doi.wiley.com/10.1029/2011JD015921, 2011.

de Boer, H. J., Eppinga, M. B., Wassen, M. J., and Dekker, S. C.: A critical transition in leaf evolution facilitated the Cretaceous angiosperm revolution, Nature Communications, 3, 1221, https://doi.org/10.1038/ncomms2217, http://www.pubmedcentral.nih.gov/articlerender.fcgi?artid=3514505{&}tool=pmcentrez{&}rendertype=abstracthttp://www.nature.com/doifinder/10.1038/ncomms2217, 2012.

Degu, A. M., Hossain, F., Niyogi, D., Pielke, R., Shepherd, J. M., Voisin, N., and Chronis, T.: The influence of large dams on surrounding climate and precipitation patterns, Geophysical Research Letters, 38, n/a–n/a, https://doi.org/10.1029/2010GL046482, http://doi.wiley.com/10.1029/2010GL046482, 2011.

Duethmann, D., Blöschl, G., and Parajka, J.: Why does a conceptual hydrological model fail to correctly predict discharge changes in response to climate change?, Hydrology and Earth System Sciences, 24, 3493–3511, https://doi.org/10.5194/hess-24-3493-2020, https://hess.copernicus.org/articles/24/3493/2020/, 2020.

Feng, X. M., Fu, B. J., Piao, S. L., Wang, S., Ciais, P., Zeng, Z. Z., Lü, Y. H., Zeng, Y., Li, Y., Jiang, X. H., and Wu, B. F.: Revegetation in China's Loess Plateau is approaching sustainable water resource limits, Nature Climate Change, 6, 1019–1022, https://doi.org/10.1038/nclimate3092, http://www.nature.com/doifinder/10.1038/nclimate3092, 2016.

Friedrich, K., Grossman, R. L., Huntington, J., Blanken, P. D., Lenters, J., Holman, K. D., Gochis, D., Livneh, B., Prairie, J., Skeie, E., Healey, N. C., Dahm, K., Pearson, C., Finnessey, T., Hook, S. J., and Kowalski, T.: Reservoir Evaporation in the Western United States: Current Science, Challenges, and Future Needs, Bulletin of the American Meteorological Society, 99, 167–187, https://doi.org/10.1175/BAMS-D-15-00224.1, http://journals.ametsoc.org/doi/10.1175/BAMS-D-15-00224.1, 2018.

Grill, G., Lehner, B., Thieme, M., Geenen, B., Tickner, D., Antonelli, F., Babu, S., Borrelli, P., Cheng, L., Crochetiere, H., Ehalt Macedo, H., Filgueiras, R., Goichot, M., Higgins, J., Hogan, Z., Lip, B., McClain, M. E., Meng, J., Mulligan, M., Nilsson, C., Olden, J. D., Opperman, J. J., Petry, P., Reidy Liermann, C., Sáenz, L., Salinas-Rodríguez, S., Schelle, P., Schmitt, R. J. P., Snider, J., Tan, F., Tockner, K., Valdujo, P. H., van Soesbergen, A., and Zarfl, C.: Mapping the world's free-flowing rivers, Nature, 569, 215–221, https://doi.org/10.1038/s41586-019-1111-9, http://www.nature.com/articles/s41586-019-1111-9, 2019.

Gupta, H. V., Kling, H., Yilmaz, K. K., and Martinez, G. F.: Decomposition of the mean squared error and NSE performance criteria: Implications for improving hydrological modelling, Journal of Hydrology, 377, 80–91, https://doi.org/10.1016/j.jhydrol.2009.08.003, http://dx.doi.org/10.1016/j.jhydrol.2009.08.003https://linkinghub.elsevier.com/retrieve/pii/S0022169409004843, 2009.

Haddeland, I., Heinke, J., Biemans, H., Eisner, S., Flörke, M., Hanasaki, N., Konzmann, M., Ludwig, F., Masaki, Y., Schewe, J., Stacke, T., Tessler, Z. D., Wada, Y., and Wisser, D.: Global water resources affected by human interventions and climate change, Proceedings of the National Academy of Sciences, 111, 3251–3256, https://doi.org/10.1073/pnas.1222475110, http://www.pnas.org/lookup/doi/10.1073/pnas.1222475110, 2014.

Hanasaki, N., Kanae, S., and Oki, T.: A reservoir operation scheme for global river routing models, Journal of Hydrology, 327, 22–41, https://doi.org/10.1016/j.jhydrol.2005.11.011, https://linkinghub.elsevier.com/retrieve/pii/S0022169405005962, 2006.

Hanasaki, N., Fujimori, S., Yamamoto, T., Yoshikawa, S., Masaki, Y., Hijioka, Y., Kainuma, M., Kanamori, Y., Masui, T., Takahashi, K., and Kanae, S.: A global water scarcity assessment under Shared Socio-economic Pathways - Part 2: Water availability and scarcity, Hydrology and Earth System Sciences, 17, 2393–2413, https://doi.org/10.5194/hess-17-2393-2013, https://www.hydrol-earth-syst-sci.net/17/2393/2013/, 2013.

Hanasaki, N., Yoshikawa, S., Pokhrel, Y., and Kanae, S.: A global hydrological simulation to specify the sources of water used by humans, Hydrology and Earth System Sciences, 22, 789–817, https://doi.org/10.5194/hess-22-789-2018, https://www.hydrol-earth-syst-sci.net/22/789/2018/, 2018.

Humphries, P., Keckeis, H., and Finlayson, B.: The River Wave Concept: Integrating River Ecosystem Models, BioScience, 64, 870–882, https://doi.org/10.1093/biosci/biu130, http://academic.oup.com/bioscience/article/64/10/870/1780369/The-River-Wave-Concept-Integrating-River-Ecosystem, 2014.

Intergovernmental Panel on Climate Change: Fifth Assessment Report of the Intergovernmental Panel on Climate Change, Tech. rep., World Meteorological Organization, 2014.

Jin, S. Y., Zhang, P., and Zhao, W. R.: Analysis of flow process variation degree and influencing factors in inner Mongolia reach of the Yellow River, IOP Conference Series: Earth and Environmental Science, 69, 012 015, https://doi.org/10.1088/1755-1315/69/1/012015, http://stacks.iop.org/1755-1315/69/i=1/a=012015?key=crossref.77e9b258768dfe7eb97dc4049c4fa6f0, 2017.

Jung, M., Reichstein, M., and Bondeau, A.: Towards global empirical upscaling of FLUXNET eddy covariance observations: Validation of a model tree ensemble approach using a biosphere model, Biogeosciences, 6, 2001–2013, https://doi.org/10.5194/bg-6-2001-2009, http://www.biogeosciences.net/6/2001/2009/, 2009.

Kim, H.: Global Soil Wetness Project Phase 3 Atmospheric Boundary Conditions (Experiment 1) [Data set], https://doi.org/10.20783/DIAS.501, 2017.

Kling, H., Fuchs, M., and Paulin, M.: Runoff conditions in the upper Danube basin under an ensemble of climate change scenarios, Journal of Hydrology, 424-425, 264–277, https://doi.org/10.1016/j.jhydrol.2012.01.011, https://linkinghub.elsevier.com/retrieve/pii/S0022169412000431, 2012.

Kobayashi, K. and Salam, M. U.: Comparing Simulated and Measured Values Using Mean Squared Deviation and its Components, Agronomy Journal, 92, 345, https://doi.org/10.1007/s100870050043, http://link.springer.de/link/service/journals/10087/bibs/0092002/00920345.htm, 2000.

Kong, D. X., Miao, C. Y., Wu, J. W., Borthwick, A. G. L., Duan, Q. Y., and Zhang, X. M.: Environmental impact assessments of the Xiaolangdi Reservoir on the most hyperconcentrated laden river, Yellow River, China, Environmental Science and Pollution Research, 24, 4337–4351, https://doi.org/10.1007/s11356-016-7975-4, http://dx.doi.org/10.1007/s11356-016-7975-4http://link.springer.com/10.1007/s11356-016-7975-4, 2017.

Kustu, M. D., Fan, Y., and Rodell, M.: Possible link between irrigation in the U.S. High Plains and increased summer streamflow in the Midwest, Water Resources Research, 47, https://doi.org/10.1029/2010WR010046, http://doi.wiley.com/10.1029/2010WR010046, 2011.

Li, C., Yang, S. Y., Lian, E. G., Yang, C. F., Deng, K., and Liu, Z. F.: Damming effect on the Changjiang (Yangtze River) river water cycle based on stable hydrogen and oxygen isotopic records, Journal of Geochemical Exploration, 165, 125–133, https://doi.org/10.1016/j.gexplo.2016.03.006, http://dx.doi.org/10.1016/j.gexplo.2016.03.006https://linkinghub.elsevier.com/retrieve/pii/S0375674216300656, 2016.

Lian, X., Piao, S. L., Li, L. Z. X., Li, Y., Huntingford, C., Ciais, P., Cescatti, A., Janssens, I. A., Peñuelas, J., Buermann, W., Chen, A. P., Li, X. Y., Myneni, R. B., Wang, X. H., Wang, Y. L., Yang, Y. T., Zeng, Z. Z., Zhang, Y. Q., and McVicar, T. R.: Summer soil drying exacerbated by earlier spring greening of northern vegetation, Science Advances, 6, https://doi.org/10.1126/sciadv.aax0255, 2020.

Liu, J. G., Zhao, D. D., Gerbens-Leenes, P. W., and Guan, D. B.: China's rising hydropower demand challenges water sector, Scientific Reports, 5, 11 446, https://doi.org/10.1038/srep11446, http://dx.doi.org/10.1038/srep11446http://www.nature.com/articles/srep11446, 2015.

Liu, J. G., Yang, H., Gosling, S. N., Kummu, M., Flörke, M., Pfister, S., Hanasaki, N., Wada, Y., Zhang, X. X., Zheng, C. M., Alcamo, J., and Oki, T.: Water scarcity assessments in the past, present, and future, Earth's Future, 5, 545–559, https://doi.org/10.1002/2016EF000518, http://doi.wiley.com/10.1002/2016EF000518, 2017.

Liu, L. L. and Du, J. J.: Documented changes in annual runoff and attribution since the 1950s within selected rivers in China, Advances in Climate Change Research, 8, 37–47, https://doi.org/10.1016/j.accre.2017.03.005, https://linkinghub.elsevier.com/retrieve/pii/S167492781630065X, 2017.

Liu, X. C., Liu, W. F., Yang, H., Tang, Q. H., Flörke, M., Masaki, Y., Müller Schmied, H., Ostberg, S., Pokhrel, Y., Satoh, Y., and Wada, Y.: Multimodel assessments of human and climate impacts on mean annual streamflow in China, Hydrology and Earth System Sciences, 23, 1245–1261, https://doi.org/10.5194/hess-23-1245-2019, https://www.hydrol-earth-syst-sci.net/23/1245/2019/, 2019.

Martens, B., Miralles, D. G., Lievens, H., van der Schalie, R., de Jeu, R. A. M., Fernández-Prieto, D., Beck, H. E., Dorigo, W. A., and Verhoest, N. E. C.: GLEAM v3: satellite-based land evaporation and root-zone soil moisture, Geoscientific Model Development, 10, 1903–1925, https://doi.org/10.5194/gmd-10-1903-2017, http://www.geosci-model-dev-discuss.net/gmd-2016-162/https://www.geosci-model-dev.net/10/1903/2017/, 2017.

Nash, J. and Sutcliffe, J.: River flow forecasting through conceptual models part I — A discussion of principles, Journal of Hydrology, 10, 282–290, https://doi.org/10.1016/0022-1694(70)90255-6, https://linkinghub.elsevier.com/retrieve/pii/0022169470902556, 1970.

Ngo-Duc, T., Laval, K., Ramillien, G., Polcher, J., and Cazenave, A.: Validation of the land water storage simulated by Organising Carbon and Hydrology in Dynamic Ecosystems (ORCHIDEE) with Gravity Recovery and Climate Experiment (GRACE) data, Water Resources Research, 43, 1–8, https://doi.org/10.1029/2006WR004941, 2007.

Piao, S., Friedlingstein, P., Ciais, P., de Noblet-Ducoudre, N., Labat, D., and Zaehle, S.: Changes in climate and land use have a larger direct impact than rising CO2 on global river runoff trends, Proceedings of the National Academy of Sciences, 104, 15 242–15 247, https://doi.org/10.1073/pnas.0707213104, http://www.pnas.org/cgi/doi/10.1073/pnas.0707213104, 2007.

Piao, S. L., Ciais, P., Huang, Y., Shen, Z. H., Peng, S. S., Li, J. S., Zhou, L. P., Liu, H. Y., Ma, Y. C., Ding, Y. H., Friedlingstein, P., Liu, C. Z., Tan, K., Yu, Y. Q., Zhang, T. Y., and Fang, J. Y.: The impacts of climate change on water resources and agriculture in China, Nature, 467, 43–51, https://doi.org/10.1038/nature09364, http://www.ncbi.nlm.nih.gov/pubmed/20811450http://www.nature.com/doifinder/10.1038/nature09364, 2010.

Ran, L. S. and Lu, X. X.: Delineation of reservoirs using remote sensing and their storage estimate: An example of the Yellow River basin, China, Hydrological Processes, 26, 1215–1229, https://doi.org/10.1002/hyp.8224, http://doi.wiley.com/10.1002/hyp.8224, 2012.

Scanlon, B. R., Zhang, Z. Z., Save, H., Sun, A. Y., Müller Schmied, H., van Beek, L. P. H., Wiese, D. N., Wada, Y., Long, D., Reedy, R. C., Longuevergne, L., Döll, P., and Bierkens, M. F. P.: Global models underestimate large decadal declining and rising water storage trends relative to GRACE satellite data, Proceedings of the National Academy of Sciences, 115, E1080–E1089, https://doi.org/10.1073/pnas.1704665115, http://www.pnas.org/lookup/doi/10.1073/pnas.1704665115, 2018.

Seneviratne, S. I., Donat, M. G., Mueller, B., and Alexander, L. V.: No pause in the increase of hot temperature extremes, Nature Climate Change, 4, 161–163, https://doi.org/10.1038/nclimate2145, http://dx.doi.org/10.1038/nclimate2145http://www.nature.com/doifinder/10.1038/nclimate2145, 2014.

Sherwood, S. and Fu, Q.: A Drier Future?, Science, 343, 737–739, https://doi.org/10.1126/science.1247620, http://www.sciencemag.org/cgi/doi/10.1126/science.1247620, 2014.

Shiklomanov, I. A.: State Hydrological Institute (SHL. St. Petersburg) and United Nations Educational, Scientific and Cultural Organisation, 1999.

Tang, Q. H., Oki, T., Kanae, S., and Hu, H. P.: Hydrological Cycles Change in the Yellow River Basin during the Last Half of the Twentieth Century, Journal of Climate, 21, 1790–1806, https://doi.org/10.1175/2007JCLI1854.1, http://journals.ametsoc.org/doi/abs/10.1175/2007JCLI1854.1, 2008.

Voisin, N., Li, H., Ward, D., Huang, M., Wigmosta, M., and Leung, L. R.: On an improved sub-regional water resources management representation for integration into earth system models, Hydrology and Earth System Sciences, 17, 3605–3622, https://doi.org/10.5194/hess-17-3605-2013, https://www.hydrol-earth-syst-sci.net/17/3605/2013/, 2013.

Wada, Y., Wisser, D., and Bierkens, M. F. P.: Global modeling of withdrawal, allocation and consumptive use of surface water and groundwater resources, Earth System Dynamics, 5, 15–40, https://doi.org/10.5194/esd-5-15-2014, http://www.earth-syst-dynam.net/5/15/2014/, 2014.

Wada, Y., de Graaf, I. E. M., and van Beek, L. P. H.: High-resolution modeling of human and climate impacts on global water resources, Journal of Advances in Modeling Earth Systems, 8, 735–763, https://doi.org/10.1002/2015MS000618, http://doi.wiley.com/10.1002/2015MS000618, 2016.

Wang, H. J., Yang, Z. S., Saito, Y., Liu, J. P., and Sun, X. X.: Interannual and seasonal variation of the Huanghe (Yellow River) water discharge over the past 50 years: Connections to impacts from ENSO events and dams, Global and Planetary Change, 50, 212–225, https://doi.org/10.1016/j.gloplacha.2006.01.005, https://linkinghub.elsevier.com/retrieve/pii/S0921818106000178, 2006.

Wang, S. S., Mo, X. G., Liu, S. X., Lin, Z. H., and Hu, S.: Validation and trend analysis of ECV soil moisture data on cropland in North China Plain during 1981–2010, International Journal of Applied Earth Observation and Geoinformation, 48, 110–121, https://doi.org/10.1016/j.jag.2015.10.010, http://www.sciencedirect.com/science/article/pii/S0303243415300441http://linkinghub.elsevier.com/retrieve/pii/S0303243415300441, 2016.

Wang, X. H.: Impacts of environmental change on rice ecosystems in China: development, optimization and application of ORCHIDEE-CROP model, Ph.D. thesis, Peking University, 2016.

Wang, X. H., Ciais, P., Li, L., Ruget, F., Vuichard, N., Viovy, N., Zhou, F., Chang, J. F., Wu, X. C., Zhao, H. F., and Piao, S. L.: Management outweighs climate change on affecting length of rice growing period for early rice and single rice in China during 1991–2012, Agricultural and Forest Meteorology, 233, 1–11, https://doi.org/10.1016/j.agrformet.2016.10.016, http://linkinghub.elsevier.com/retrieve/pii/S0168192316304087, 2017.

Wang, X. J., Engel, B., Yuan, X. M., and Yuan, P. X.: Variation Analysis of Streamflows from 1956 to 2016 Along the Yellow River, China, Water, 10, 1231, https://doi.org/10.3390/w10091231, http://www.mdpi.com/2073-4441/10/9/1231, 2018.

Wu, X. C., Vuichard, N., Ciais, P., Viovy, N., de Noblet-Ducoudré, N., Wang, X. H., Magliulo, V., Wattenbach, M., Vitale, L., Di Tommasi, P., Moors, E. J., Jans, W., Elbers, J., Ceschia, E., Tallec, T., Bernhofer, C., Grünwald, T., Moureaux, C., Manise, T., Ligne, A., Cellier, P., Loubet, B., Larmanou, E., and Ripoche, D.: ORCHIDEE-CROP (v0), a new process-based agro-land surface model: model description and evaluation over Europe, Geoscientific Model Development, 9, 857–873, https://doi.org/10.5194/gmd-9-857-2016, http://www.geosci-model-dev-discuss.net/8/4653/2015/http://www.geosci-model-dev.net/9/857/2016/, 2016.

Xi, Y., Peng, S. S., Ciais, P., Guimberteau, M., Li, Y., Piao, S. L., Wang, X. H., Polcher, J., Yu, J. S., Zhang, X. Z., Zhou, F., Bo, Y., Ottle, C., and Yin, Z.: Contributions of Climate Change, CO 2 , Land-Use Change, and Human Activities to Changes in River Flow across 10 Chinese Basins, Journal of Hydrometeorology, 19, 1899–1914, https://doi.org/10.1175/JHM-D-18-0005.1, http://journals.ametsoc.org/doi/10.1175/JHM-D-18-0005.1, 2018.

Yaghmaei, H., Sadeghi, S. H., Moradi, H., and Gholamalifard, M.: Effect of Dam operation on monthly and annual trends of flow discharge in the Qom Rood Watershed, Iran, Journal of Hydrology, 557, 254–264, https://doi.org/10.1016/j.jhydrol.2017.12.039, http://linkinghub.elsevier.com/retrieve/pii/S0022169417308570, 2018.

Yin, Z.: yinzun2000/Irrig_Dam_YellowRiver_HESS: Code and data for "Irrigation, damming, and streamflow fluctuations of the Yellow River", https://doi.org/10.5281/zenodo.3979053, https://doi.org/10.5281/zenodo.3979053, 2020.

Yin, Z., Ottlé, C., Ciais, P., Guimberteau, M., Wang, X. H., Zhu, D., Maignan, F., Peng, S. S., Piao, S. L., Polcher, J., Zhou, F., and Kim, H.: Evaluation of ORCHIDEE-MICT-simulated soil moisture over China and impacts of different atmospheric forcing data, Hydrology and Earth System Sciences, 22, 5463–5484, https://doi.org/10.5194/hess-22-5463-2018, https://www.hydrol-earth-syst-sci-discuss.net/hess-2017-699/https://www.hydrol-earth-syst-sci.net/22/5463/2018/, 2018.

Yin, Z., Wang, X. H., Ottlé, C., Zhou, F., Guimberteau, M., Polcher, J., Peng, S. S., Piao, S. L., Li, L., Bo, Y., Chen, X. L., Zhou, X. D., Kim, H., and Ciais, P.: Improvement of the Irrigation Scheme in the ORCHIDEE Land Surface Model and Impacts of Irrigation on Regional Water Budgets Over China, Journal of Advances in Modeling Earth Systems, 12, 1–20, https://doi.org/10.1029/2019MS001770, https://onlinelibrary.wiley.com/doi/abs/10.1029/2019MS001770, 2020.

YRCC: Yellow River Water Resources Bulletin 1998–2014, Tech. rep., Yellow River Conservancy Commission, Zhengzhou, http://www.yrcc.gov.cn/other/hhgb/, 1998–2014.

Yuan, X., Ma, F., Wang, L. Y., Zheng, Z. Y., Ma, Z. G., Ye, A. Z., and Peng, S. M.: An experimental seasonal hydrological forecasting system over the Yellow River basin – Part 1: Understanding the role of initial hydrological conditions, Hydrology and Earth System Sciences, 20, 2437–2451, https://doi.org/10.5194/hess-20-2437-2016, 2016.

Yuan, X., Jiao, Y., Yang, D., and Lei, H.: Reconciling the Attribution of Changes in Streamflow Extremes From a Hydroclimate Perspective, Water Resources Research, 54, 3886–3895, https://doi.org/10.1029/2018WR022714, 2018.

Zeng, Z. Z., Wang, T., Zhou, F., Ciais, P., Mao, J. F., Shi, X. Y., and Piao, S. L.: A worldwide analysis of spatiotemporal changes in water balance-based evapotranspiration from 1982 to 2009, Journal of Geophysical Research: Atmospheres, 119, 1186–1202, https://doi.org/10.1002/2013JD020941, http://doi.wiley.com/10.1002/2013JD020941, 2014.

Zhou, F., Bo, Y., Ciais, P., Dumas, P., Tang, Q. H., Wang, X. H., Liu, J. G., Zheng, C. M., Polcher, J., Yin, Z., Guimberteau, M., Peng, S. S., Ottlé, C., Zhao, X. N., Zhao, J. S., Tan, Q., Chen, L., Shen, H. Z., Yang, H., Piao, S. L., Wang, H., and Wada, Y.: Deceleration of China's human water use and its key drivers, Proceedings of the National Academy of Sciences, 117, 7702–7711, https://doi.org/10.1073/pnas.1909902117, http://www.pnas.org/lookup/doi/10.1073/pnas.1909902117, 2020.

Zhu, Z. C., Piao, S. L., Myneni, R. B., Huang, M. T., Zeng, Z. Z., Canadell, J. G., Ciais, P., Sitch, S., Friedlingstein, P., Arneth, A., Cao, C. X., Cheng, L., Kato, E., Koven, C., Li, Y., Lian, X., Liu, Y. W., Liu, R., Mao, J. F., Pan, Y. Z., Peng, S. S., Peñuelas, J., Poulter, B., Pugh, T. A. M., Stocker, B. D., Viovy, N., Wang, X. H., Wang, Y. P., Xiao, Z. Q., Yang, H., Zaehle, S., and Zeng, N.: Greening of the Earth and its drivers, Nature Climate Change, 6, 791–795, https://doi.org/10.1038/nclimate3004, http://www.nature.com/doifinder/10.1038/nclimate3004, 2016.

Zhuo, L., Hoekstra, A. Y., Wu, P., and Zhao, X. N.: Monthly blue water footprint caps in a river basin to achieve sustainable water consumption: The role of reservoirs, Science of the Total Environment, 650, 891–899, https://doi.org/10.1016/j.scitotenv.2018.09.090, https://doi.org/10.1016/j.scitotenv.2018.09.090, 2019.

Zobler, L.: A world soil file for global climate modeling, Tech. rep., NASA Tech, 1986.

Zscheischler, J., Westra, S., van den Hurk, B. J. J. M., Seneviratne, S. I., Ward, P. J., Pitman, A., AghaKouchak, A., Bresch, D. N., Leonard, M., Wahl, T., and Zhang, X. B.: Future climate risk from compound events, Nature Climate Change, 8, 469–477, https://doi.org/10.1038/s41558-018-0156-3, http://dx.doi.org/10.1038/s41558-018-0156-3http://www.nature.com/articles/s41558-018-0156-3, 2018.

Tables

Table 1. Information of artificial reservoirs on the YR with considerable total capacity. Data is mainly from the YR Conservancy Commission of the Ministry of Water Resources (http://www.yrcc.gov.cn). The "regulation purposes" follows the style of Hanasaki et al. (2006). "H" indicates hydropower; "C" indicates flood control; "I" indicates irrigation; "W" indicates water supply; and "S" indicates scouring sediment.

Name	Total capacity (10^8 m^3)	Regulation capacity (10^8 m^3)	Regulation since	Regulation type	Regulation purposes
LongYangXia	247	193.53	Oct 1986	Inter-annual	HCIW
LiJiaXia	16.5	–	Dec 1996	Daily, weekly	HI
GongBoXia	6.2	0.75	Aug 2004	Daily	HCIW
LiuJiaXia	57	41.5	Oct 1968	Inter-annual	HCIW
YanGuoXia	2.2	–	Mar 1961	Daily	HI
BaPanXia	0.49	0.09	–	Daily	HIW
QingTongXia	$6.06 \rightarrow 0.4^*$	–	1968	Daily	HI
XiaoLangDi	126.5	91.5	1999	Inter-annual	CSWIH

* The total capacity shrink is due to sedimentation.

Table 2. Definitions of sub-sections and values of C_{dam} used in the dam regulation simulation.

Sub-section	Stations	C_{dam} (10^8 m^3)	Regulation since
R_1	– TangNaiHai	–	–
R_2	TangNaiHai LanZhou	41.5 before 1987; 235 after 1987	1982
R_3	LanZhou TouDaoGuai	–	1982
R_4	TouDaoGuai HuaYuanKou	91.5	1999
R_5	HuaYuanKou LiJin	–	–

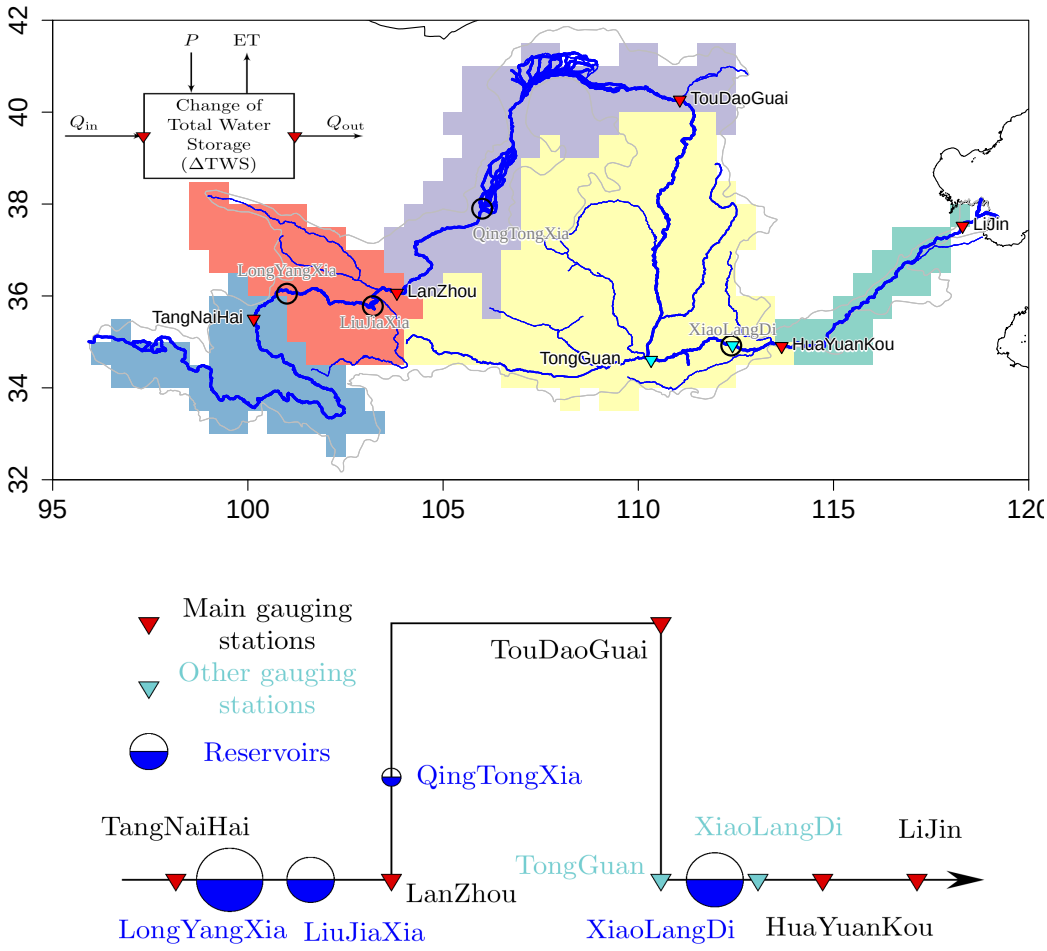

Figure 1. Top panel: map of YRB. Gray and blue lines indicate the catchment and network of YR based on GIS data, respectively. Dark circles are main artificial reservoirs on the YR. Triangles are gauging stations. Red triangles are main stations used for classifying sub-section and simulation comparison, and teal triangles are stations used to assess the impacts of XiaoLangDi Reservoir on river discharge. Colored patterns are sub-sections between two neighbouring gauging stations based on ORCHIDEE routing map. The water balances of specific sub-section are shown at the top left. Bottom panel: conceptual figure of YR main stream, gauging stations, and artificial reservoirs. The sizes of circles indicate the regulation capacities of these reservoirs (Table 2).

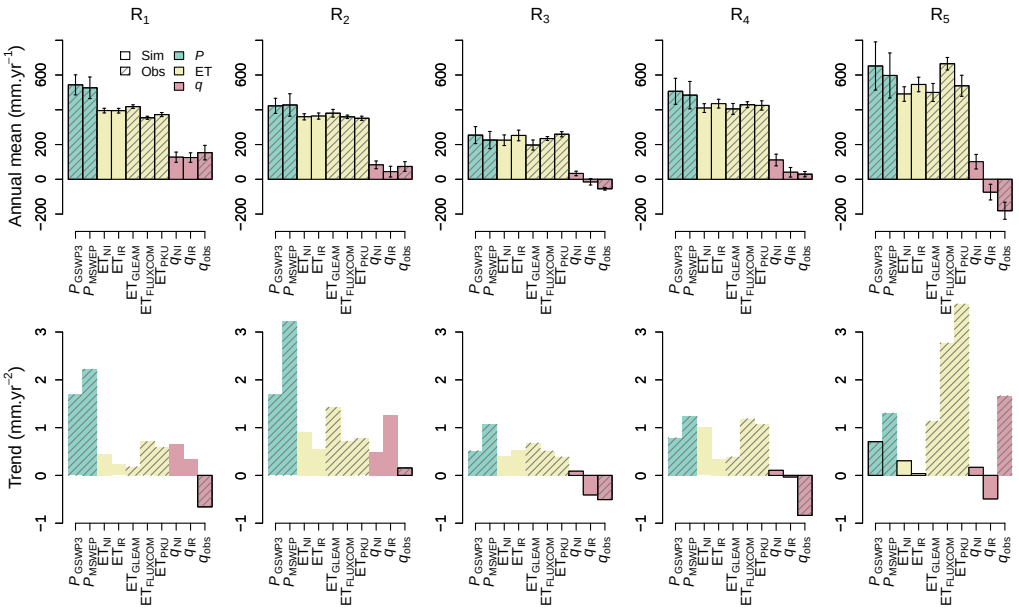

Figure 2. Top panel: Annual mean of hydrological elements in each sub-section of the YR basin from both simulation (plain colors) and observation (hatched colors). Error bars represent for standard deviation. Bottom panel: trends of these elements in each sub-section. Dark borders indicate the trend is statistical significant (p-value < 0.05) according to Mann-Kendall test.

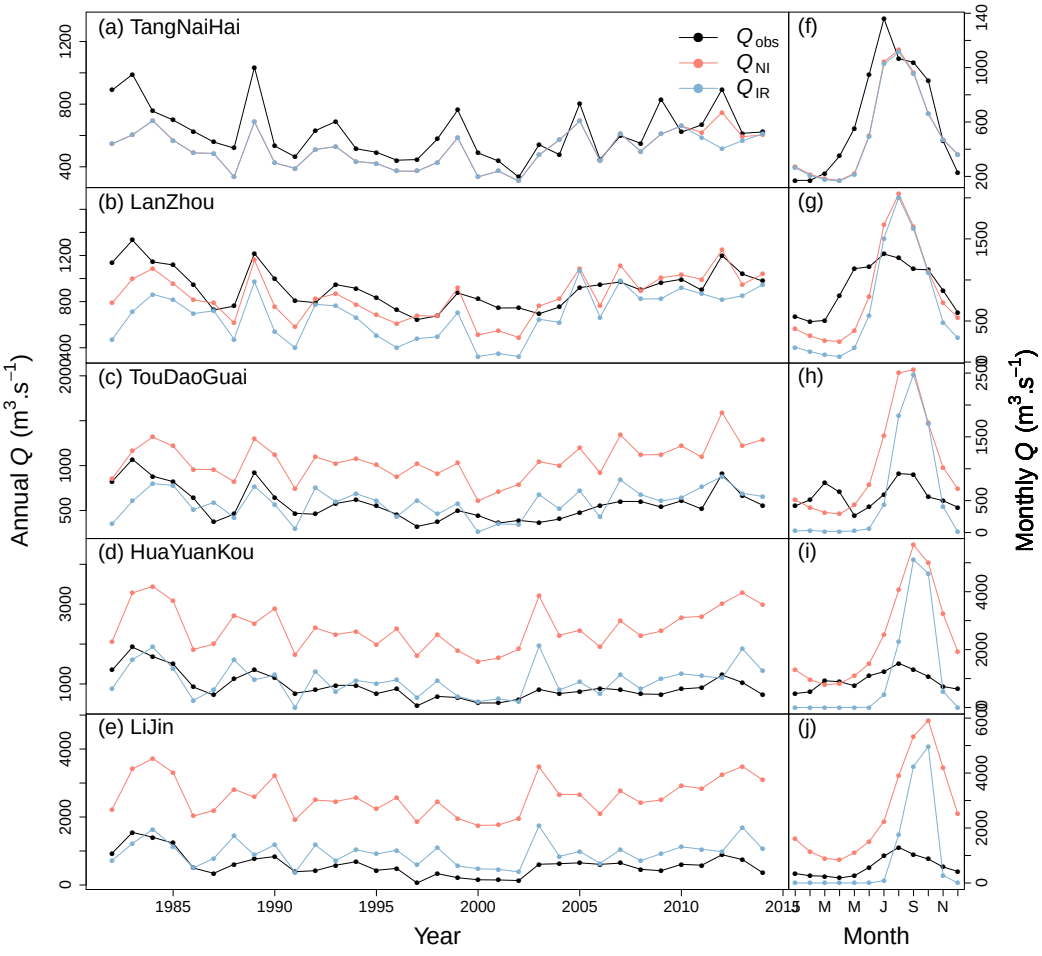

Figure 3. (a)-(e): Time series of annual discharge from observations and simulations at each gauging station. (f)-(j): Seasonality of observed and simulated discharge at each gauging station. Q_{obs} is the observed annual mean discharge. Q_{NI} and Q_{IR} are the simulated annual mean discharges based on the NI and IR simulations (Sect. 2.4), respectively. These simulations do not account for dams and therefore the seasonality has a higher amplitude than observed in the right hand plots.

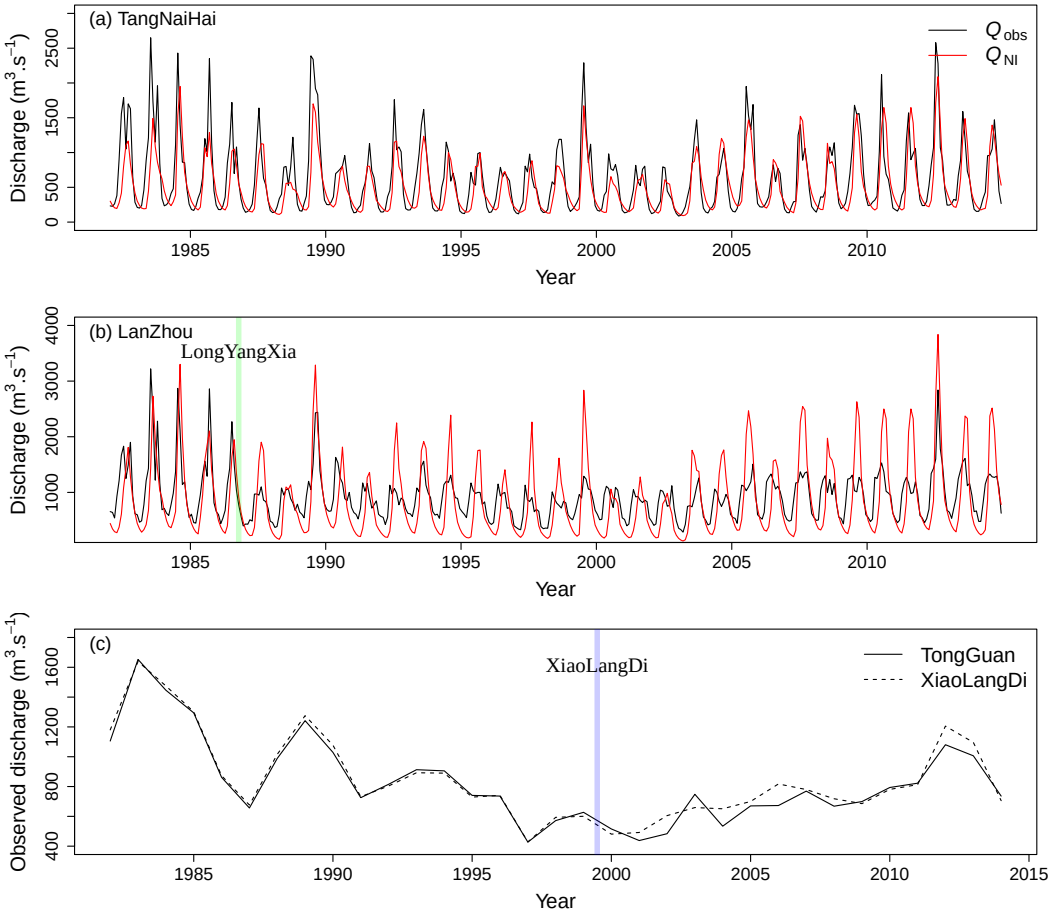

Figure 4. (a)-(b): monthly observed (Q_{obs}) and simulated (Q_{NI}) discharges at TangNaiHai and LanZhou stations. Green bar in (b) indicates the start of the LongYangXia dam regulation. (c): Observed annual discharges at TongGuan and XiaoLangDi gauging stations, which locate at up and down stream of the XiaoLangDi reservoir, respectively (see Fig. 1). Blue bar in (c) indicates the start of the XiaoLangDi dam regulation.

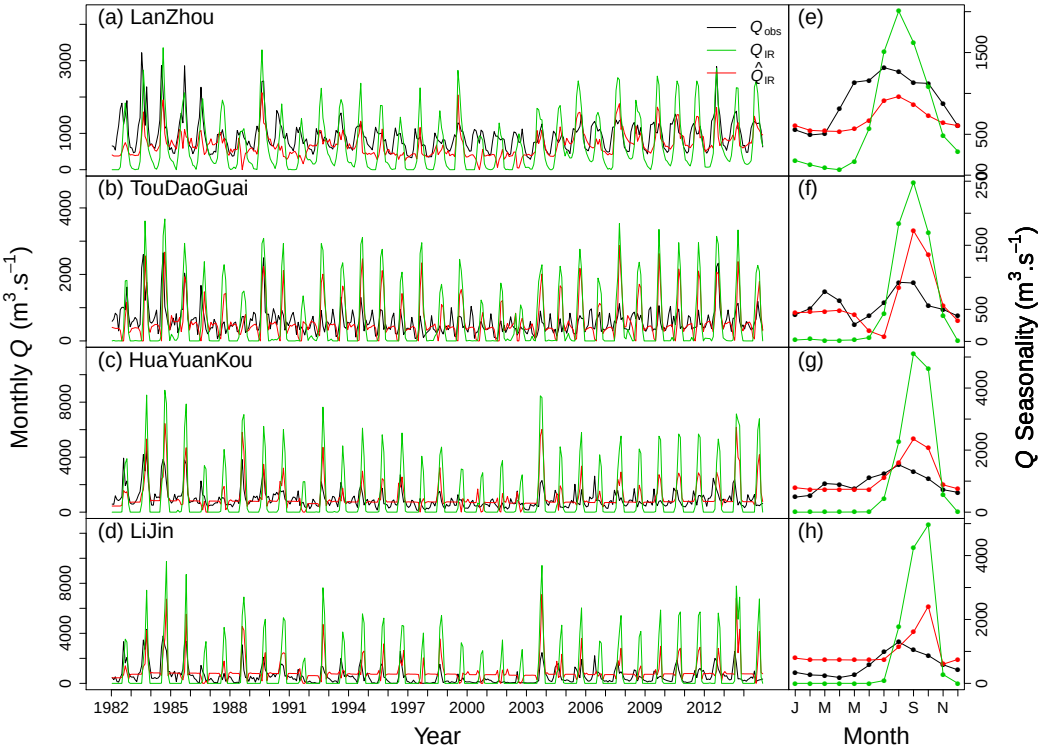

Figure 5. Comparison between observed and simulated actual monthly discharge at gauging stations. Q_{obs} (dark lines) is observed monthly discharge. Q_{IR} (green lines) is simulated monthly discharge from the IR experiment (Sect. 2.4). $\hat{Q}_{\text{IR}}$ (red lines) is simulated monthly discharge including impacts of reservoir regulation (Sect. 2.4).

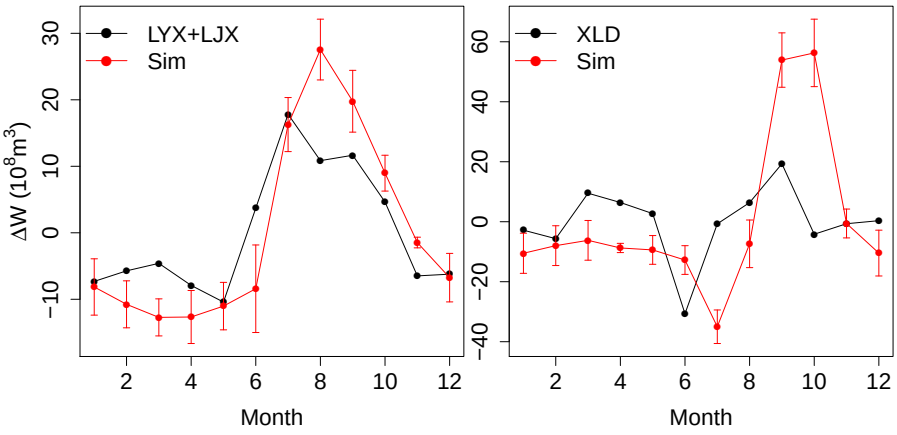

Figure 6. The changes of water storage of dams (ΔW) in R_2 and R_4. The dark line represents the ΔW from literature. The multi-year mean of ΔW of LongYangXi and LiuJiaXia is from Jin et al. (2017). The ΔW of XiaoLangDi is from one-year record reported in Kong et al. (2017). Red lines represent corresponding simulated ΔW from our dam regulation model.

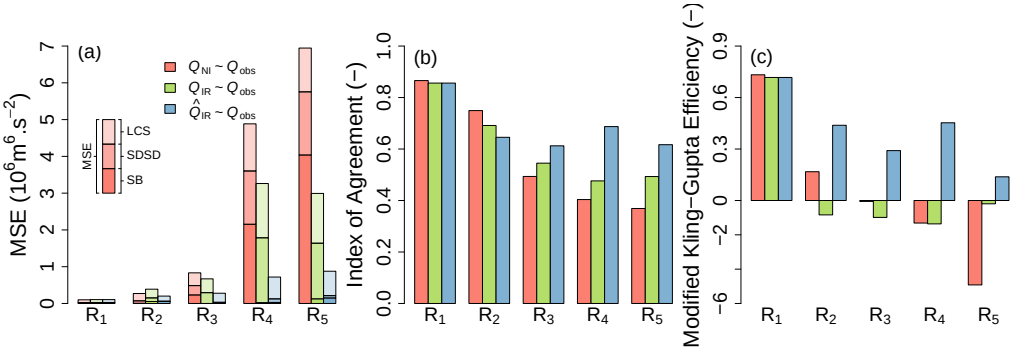

Figure 7. Indicators of Q comparisons in each sub-section of YRB. Colors indicate different comparisons. The MSE is decomposed to SB, SDSD, and LCS, which are distinguished by different transparencies.